Optical Vector Network Analyzer Based on Unbalanced Double-Sideband Modulation

Muguang Wang, *Member, IEEE*, and Jianping Yao, *Fellow, IEEE*

***Abstract*— An optical vector network analyzer (OVNA) based on unbalanced double-sideband (UB-DSB) modulation with improved measurement accuracy is proposed and experimentally demonstrated. It is different from an OVNA based on optical single-sideband (OSSB) modulation in which one-to-one mapping between the optical and radio frequency responses is employed to measure the magnitude and phase responses of an optical component, the proposed technique measures the magnitude and phase responses by taking into consideration of the power of the other sideband through solving two equations that are associated with the UB-DSB modulation, thus the errors due to the residual power of the other sideband in an OSSB modulation based approach are completely eliminated. A mathematical model providing the transfer function of an optical component is derived. The measurement of a phase-shifted fiber Bragg grating and a linearly chirped fiber Bragg grating is performed. Comparing with the measured results based on OSSB modulation, obvious improvement in measurement accuracy is demonstrated.**

***Index Terms*— Fiber Bragg grating, microwave photonics, optical fiber measurements, single sideband modulation, unbalanced double-sideband modulation.**

I. Introduction

THE magnitude and phase responses of an optical component are usually measured using an optical vector network analyzer (OVNA). It is highly desirable that an OVNA can perform spectrum measurement with high accuracy. It is also expected that an OVNA can operate over a broad bandwidth. In general, two techniques have been proposed to characterize an optical component: the modulation phase-shift technique [1], [2] and the interferometry technique [3], [4]. Although significant progress has been made in the last few years, the performance of an OVNA, especially the spectral accuracy, still has room to improve. Numerous techniques have recently been proposed and demonstrated. In [5], an OVNA based on optical single-sideband (OSSB) modulation was proposed. The optical magnitude and phase responses were characterized by measuring the RF current at the output of a photodetector (PD). Due to the OSSB modulation [6], one-to-one mapping between the optical and RF responses is achieved. Since the RF frequency can be tuned with a resolution in Hertz, an extremely high spectral resolution is achievable. The key to implement the technique with high accuracy is to ensure an ideal OSSB modulation, to eliminate completely the other sideband. However, OSSB modulation using a dual-port Mach–Zehnder modulator (MZM) [7] or a bidirectional single-electrode MZM [8] cannot provide ideal OSSB modulation due to the fact that the optical power splitting ratio between the two arms of an MZM cannot be precisely controlled identical. The residual power from the other sideband will destroy the one-to-one mapping relationship and lead to reduced measurement accuracy. It has been analyzed that a residual power of -10 dB relative to the wanted sideband will lead to a magnitude error of 3 dB [9]. In addition, OSSB modulation using a dual-port MZM or a bidirectional single-electrode MZM has a limited bandwidth due to the use of a band-limited 90° RF hybrid, which will restrain the operation bandwidth of an OVNA. To increase the bandwidth, recently an OVNA using a tunable optical filter with two highly steep edges and a flat-top to achieve wideband OSSB modulation was demonstrated [10]. A bandwidth as large as 40 GHz was realized. The limitation of the technique again is the relatively poor accuracy due to the residual power of the other sideband. Although the tunable optical filter has an edge slope as steep as 230 dB/nm, the power ratio between the unwanted and wanted sidebands is only 20 dB, leading to an error of about 1 dB.

In this letter, we propose a novel technique to implement an OVNA based on unbalanced double-sideband (UB-DSB) modulation with improved accuracy. Instead of measuring the magnitude and phase responses of an optical component based on the one-to-one mapping, the spectral responses are measured by taking into consideration of the power of the other sideband through solving two equations that are associated with the UB-DSB modulation. Since the powers of the two sidebands are known, the solution of the two equations would provide the transfer function of the optical component. The proposed technique is theoretically studied and a mathematical model providing the transfer function of the optical component under test is derived. An experiment is then performed. In the experiment, the UB-DSB modulation is realized by a joint use of an MZM and an optical filter. The measurement of a phase-shifted fiber Bragg grating

Manuscript received November 14, 2012; revised January 22, 2013; accepted February 21, 2013. Date of publication February 25, 2013; date of current version March 29, 2013. This work was supported in part by the Natural Science and Engineering Research Council of Canada. The work of M. Wang was supported in part by the National Natural Science Foundation of China under Grant 60807003 and in part by the Program for New Century Excellent Talents in University under Grant NCET-09-0209.

M. Wang is with the Institute of Lightwave Technology, Key Lab of All Optical Network and Advanced Telecommunication Network of EMC, Beijing Jiaotong University, Beijing 100044, China, and also with the Microwave Photonics Research Laboratory, School of Electrical Engineering and Computer Science, University of Ottawa, Ottawa, ON K1N 6N5, Canada (e-mail: mgwang@bjtu.edu.cn).

J. Yao is with the Microwave Photonics Research Laboratory, School of Electrical Engineering and Computer Science, University of Ottawa, Ottawa, ON K1N 6N5, Canada (e-mail: jpyao@eecs.uottawa.ca).

Color versions of one or more of the figures in this letter are available online at http://ieeexplore.ieee.org.

Digital Object Identifier 10.1109/LPT.2013.2249058

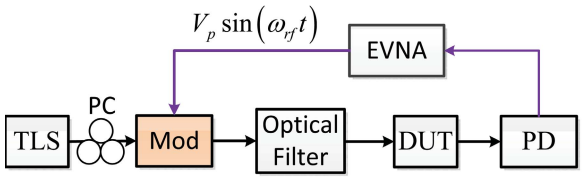

Fig. 1. Schematic diagram of the proposed optical vector network analyzer.

(PS-FBG) and a linearly chirped fiber Bragg grating (LC-FBG) is performed. Comparing with the results based on the OSSB modulation based technique with a sideband suppression radio (SSR) of 10 and 20 dB, an obvious improvement in measurement accuracy is demonstrated.

II. Principle

The fundamental principle of our proposed OVNA can be explained by considering the schematic shown in Fig. 1. A CW light wave at a frequency of ω_c from a tunable laser source (TLS) is modulated by a RF signal at a frequency ω_{rf} to achieve optical double-sideband (ODSB) modulation. Under small signal modulation condition, the ODSB modulated signal can be written as [5]

$$E_{\text{mod}}(t) = A_{-1} e^{j(\omega_c - \omega_{rf})t} + A_0 e^{j\omega_c t} + A_1 e^{j(\omega_c + \omega_{rf})t} \quad (1)$$

where A_{-1}, A_0, and A_1 are the complex amplitudes of the lower first-order sideband at $\omega_c - \omega_{rf}$, the optical carrier at ω_c and the upper sideband at $\omega_c + \omega_{rf}$. Note that the modulator can be an MZM, a phase modulator (PM) or a polarization modulator (PolM). Generally, the amplitudes of the two sidebands always maintain a conjugate relation, i.e., $A_{-1}^* = A_1$. If an MZM with a zero chirp is used, the amplitudes $A_{0,\pm 1}$ would be purely real. If a PM is used, the amplitudes $A_{\pm 1}$ would be complex and A_0 would be real. Assuming that a device under test (DUT) has a frequency response of $H(\omega)$, the optical field at the output of the DUT can be expressed as

$$\begin{aligned} E_{\text{DUT}}(\omega) = 2\pi \big[& A_{-1} H(\omega_c - \omega_{rf}) \delta(\omega - \omega_c + \omega_{rf}) \\ & + A_0 H(\omega_c) \delta(\omega - \omega_c) + A_1 H(\omega_c + \omega_{rf}) \\ & \delta(\omega - \omega_c - \omega_{rf}) \big] \end{aligned} \quad (2)$$

The optical signal is then detected by a PD, and the photocurrent at the RF frequency is given by

$$\begin{aligned} i(\omega_{rf}) \propto & A_0 A_{-1}^* H^*(\omega_c - \omega_{rf}) H(\omega_c) \\ & + A_0 A_1 H^*(\omega_c) H(\omega_c + \omega_{rf}) \end{aligned} \quad (3)$$

where * represents the complex conjugation. If OSSB modulation is employed, one of the two terms at the right side of (3) would be zero, and the transfer function $H(\omega_c + \omega_{rf})$ or $H^*(\omega_c - \omega_{rf})$ of the DUT can be fully determined based on the detected electrical signal, that is,

$$H(\omega_c + \omega_{rf}) \propto \frac{i(\omega_{rf})}{A_0 A_1 H^*(\omega_c)} \text{ Assuming } A_{-1} = 0 \quad (4)$$

or

$$H^*(\omega_c - \omega_{rf}) \propto \frac{i(\omega_{rf})}{A_0 A_{-1}^* H(\omega_c)} \text{ Assuming } A_1 = 0. \quad (5)$$

For practical implementation, however, an ideal OSSB modulation with a completely suppressed other sideband is hard to achieve. The residual power from the other sideband would introduce measurement errors [9]. To precisely measure, the residual power from the other sideband must be considered. Here we propose a novel technique based on UB-DSB modulation to precisely measure the transfer function of the DUT. The UB-DSB modulation is realized based on an MZM to generate a balanced DSB modulated signal followed by an optical filter with its central wavelength located at one sideband to attenuate part of the sideband. As shown in Fig. 1, the balanced DSB modulated signal is sent to a reconfigurable optical filter to impose two different attenuations to the sideband. Then the optical signal is injected into the DUT. By measuring the detected electrical signals using an electrical vector network analyzer (EVNA) twice, a matrix equation is built, and the transfer function from the measured electrical signals can be solved. The photocurrents when the optical filter is configured with two different attenuations are given by

$$\begin{bmatrix} i_1(\omega_{rf}) \\ i_2(\omega_{rf}) \end{bmatrix} \propto \begin{bmatrix} w_1 A_0 A_{-1}^* H(\omega_c) & A_0 A_1 H^*(\omega_c) \\ w_2 A_0 A_{-1}^* H(\omega_c) & A_0 A_1 H^*(\omega_c) \end{bmatrix} \begin{bmatrix} H^*(\omega_c - \omega_{rf}) \\ H(\omega_c + \omega_{rf}) \end{bmatrix} \quad (6)$$

where $i_1(\omega_{rf})$ and $i_2(\omega_{rf})$ are the two detected photocurrents, and w_1 and w_2 represents the corresponding two attenuations. The key of this technique is that the ratio of the transfer functions of the two measurements at the lower sideband is different from that at the upper sideband, so that the determinant of the matrix is nonzero, and the frequency responses of the DUT at $\omega_c + \omega_{rf}$ and $\omega_c - \omega_{rf}$ are given by

$$H(\omega_c + \omega_{rf}) = \frac{w_2 i_1(\omega_{rf}) - w_1 i_2(\omega_{rf})}{(w_2 - w_1) A_0 A_1 H^*(\omega_c)} \quad (7.1)$$

$$H^*(\omega_c - \omega_{rf}) = \frac{i_1(\omega_{rf}) - i_2(\omega_{rf})}{(w_1 - w_2) A_0 A_{-1}^* H^*(\omega_c)} \quad (7.2)$$

Since w_1 and w_2 are known, $H(\omega_c)$ is a complex constant, and the complex amplitude $A_{0,\pm 1}$ can be obtained by a calibration process, by sweeping ω_{rf} using an EVNA, the frequency response of the DUT can thus be measured accurately.

III. Experimental Results

An experiment based on the setup shown in Fig. 2 is performed. The light wave from a TLS (Agilent N7714A) is sent to a PolM. The TLS has a wavelength tunable range of 38 nm (1527 to 1565 nm), a linewidth of less than 100 kHz and a 24-hour wavelength drift of less than 2.5 pm. The PolM is a special phase modulator that supports phase modulation along the two principal axes with opposite phase modulation indices [11]. The joint operation of the PolM, a polarization controller (PC), and a polarizer corresponds to an intensity modulator. A fully programmable optical filter (Finisar WaveShaper 4000S) with independently tunable center wavelength, bandwidth and attenuation is employed to serve as the reconfigurable optical filter. A wideband PD (u^2t XPDV2150R) with

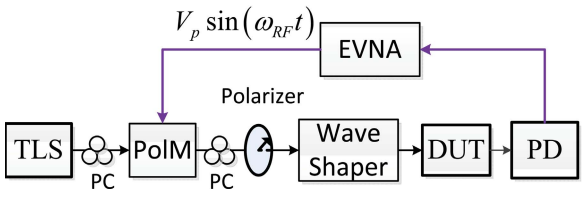

Fig. 2. Experimental setup of the proposed OVNA.

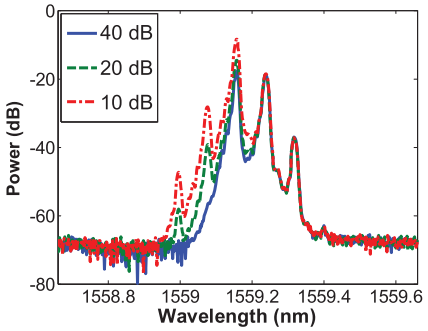

Fig. 3. Optical spectra of the UB-DSB modulated signals with different SSRs of 10, 20, and 40 dB.

a bandwidth of 50 GHz and a responsivity of 0.65 A/W is employed to convert the optical signal to an electrical signal, and the spectral response is measured by an EVNA (Agilent E8364A).

First, UB-DSB modulation is experimented. To do so, the WaveShaper is configured by setting its stopband at one sideband of the modulated signal, the SSR is controlled by adjusting the attenuation of the WaveShaper to have different attenuations of 10, 20 and 40 dB. Fig. 3 shows the optical spectra of the optical UB-DSB modulated signal after passing through the WaveShaper. In the experiment, the optical carrier is set at 1559.16 nm, and the RF signal is set at 10 GHz. As can be seen, the UB-DSB modulation is close to an ideal OSSB modulation when the SSR is 40 dB.

Then, the measurement of the spectral response of an ultra-narrow PS-FBG is performed. First, we measure the magnitude and phase responses based on the OSSB modulation technique, where the SSR is controlled at 10, 20 and 40 dB. The results are shown in Fig. 4. It is clearly seen that the measurement errors are increased at the notch of the PS-FBG when the SSR is decreased. The measurement errors, taking the magnitude response based on the OSSB modulation for the SSR of 40 dB as a reference, are calculated, which are 8.1 dB and 1.9 dB when the SSR are 10 dB and 20 dB. Then, the magnitude and phase responses are calculated based on the proposed UB-DSB modulation technique, where the photocurrents corresponding to the SSR values of 10 and 20 dB are employed. The results are also shown in Fig. 4 (red-dot curve). As can be seen, the magnitude and phase responses based on the proposed UB-DSB modulation technique overlap with those based on the OSSB modulation technique when the SSR is 40 dB (black dash-dot curve). This confirms that the use of the UB-DSB modulation technique can achieve the same measurement accuracy as an ideal OSSB modulation technique. The magnitude and phase responses of the PS-FBG

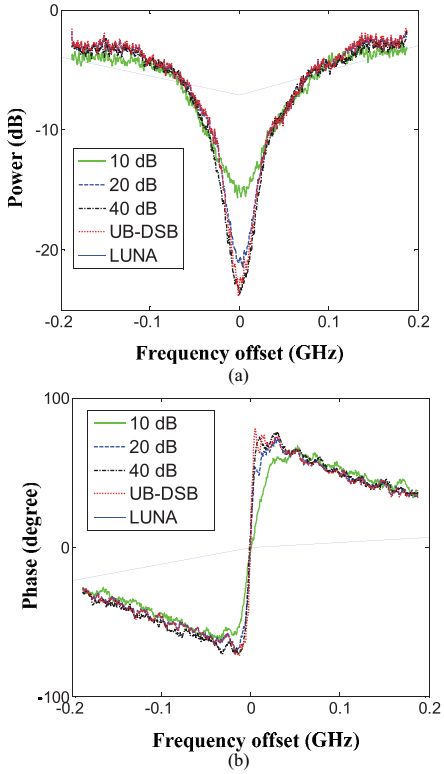

Fig. 4. Measured (a) magnitude and (b) phase responses of the PS-FBG.

are also measured using a commercial OVNA (LUNA CTe OVA 4000), with the results also shown in Fig. 4 (blue-solid curve). It can be seen for the LUNA CTe OVA (performing measurement based on interferometry method), there are only three effective measured points in the range of 0.4 GHz, and the frequency resolution is 0.2 GHz. While for the OVNA based on UB-DSB modulation or OSSB modulation, there are 1201 measured points in the range of 0.4 GHz, and the frequency resolution is 333 kHz, which is much higher than that of the commercial OVNA.

Then, the use of the proposed UB-DSB modulation technique to measure the spectral response of an LC-FBG is performed. Fig. 5(a) shows the normalized magnitude response over a frequency band of 20 GHz centered at 1558.998 nm in the passband of the LC-FBG. Although the LC-FBG has a flat passband as shown in Fig. 5(b) (a zoom-in view is given in the inset), which is measured by using a high resolution optical spectrum analyzer (OSA), the amplitude response measured by the OSSB modulation technique, especially for the SSR at 10 and 20 dB, has obvious ripples, due to the errors resulted from the residual power of the other sideband. As can be seen, the ripples decrease when the SSR increases, which has been theoretically analyzed by [9]. The magnitude response using the proposed UB-DSB modulation technique by using the photocurrents corresponding to the SSR values of 10 and 20 dB is calculated and is shown in Fig. 5(a), as the red-dot curve. The results are close to those measured by the OSSB modulation technique when the SSR is 40 dB (black dash-dot curve). Comparing with the measured results with an SSR of 10 and 20 dB, an improvement in measured accuracy by 2.8 and 1 dB, respectively, is obtained. Therefore, it confirms

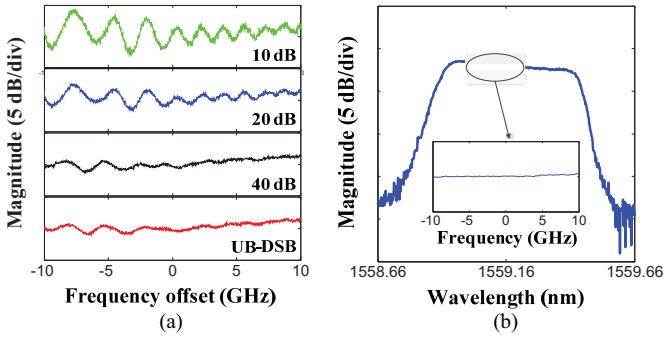

Fig. 5. (a) Measured magnitude response of the LC-FBG based on the OSSB modulation technique with an SSR of 10, 20, and 40 dB, and based on the UB-DSB modulation technique. (b) Optical spectrum of the LC-FBG measured using an OSA. Inset: zoom-in view of the optical spectrum.

again that the measurement errors due to the residual power from the other sideband of an OSSB modulated signal can be eliminated by using the proposed UB-DSB modulation technique.

IV. Discussion and Conclusion

Note that broad bandwidth measurement with high accuracy can be performed by tuning the wavelength of the TLS and the corresponding center wavelength of the optical filter. The bandwidth of the EVNA determines the measurement bandwidth at a given optical wavelength. The entire spectral response of the DUT is obtained by combining the individual measurements at all the optical wavelengths.

Note also that the measurement resolution can be improved if the TLS is locked to the EVNA. As it was demonstrated in [12], where the measurement of the mode spacing of a high finesse cavity was performed, a sub-Hertz resolution was achieved.

In summary, an OVNA with improved measurement accuracy based on UB-DSB modulation was proposed and experimentally demonstrated. Instead of measuring the magnitude and phase responses of an optical component based on the OSSB modulation technique where one-to-one mapping of the optical and electrical spectral responses is employed, the spectral responses were measured by taking into consideration of the power of the other sideband through solving two equations that were associated with the UB-DSB modulation. The proposed technique was verified experimentally. The spectral responses of two optical components, a PS-FBG and an LCFBG, were measured. The results show that the measurement accuracy was increased when compared with the OSSB modulation technique for an SSR of 10 and 20 dB.

References

[1] S. Ryu, Y. Horiuchi, and K. Mochizuki, "Novel chromatic dispersion measurement method over continuous Gigahertz tuning range," *J. Lightw. Technol.*, vol. 7, no. 8, pp. 1177–1180, Aug. 1989.

[2] T. Niemi, M. Uusimaa, and H. Ludvigsen, "Limitations of phase-shift method in measuring dense group delay ripple of fiber Bragg gratings," *IEEE Photon. Technol. Lett.*, vol. 13, no. 12, pp. 1334–1336, Dec. 2001.

[3] M. Froggatt, E. Moore, and M. Wolfe, "Interferometric measurement of dispersion in optical components," in *Proc. Opt. Fiber Commun. Conf. Exhibit.*, Mar. 2002, pp. 252–253, paper WK1.

[4] G. D. VanWiggeren, A. R. Motamedi, and D. M. Baney, "Single-scan interferometric component analyzer," *IEEE Photon. Technol. Lett.*, vol. 15, no. 2, pp. 263–265, Feb. 2003.

[5] J. E. Román, M. Y. Frankel, and R. D. Esman, "Spectral characterization of fiber gratings with high resolution," *Opt. Lett.*, vol. 23, no. 12, pp. 939–941, Jun. 1998.

[6] A. Loayssa, R. Hernandez, and D. Benito, "Optical single-side band modulators and their applications," *Fiber Integr. Opt.*, vol. 23, nos. 2–3, pp. 171–188, Mar./Jun. 2004.

[7] G. H. Smith, D. Novak, and Z. Ahmed, "Technique for optical SSB generation to overcome dispersion penalties in fibre-radio systems," *Electron. Lett.*, vol. 33, no. 1, pp. 74–75, Jan. 1997.

[8] A. Loayssa, D. Benito, and M. J. Garde, "Single-sideband suppressed-carrier modulation using a single-electrode electrooptic modulator," *IEEE Photon. Technol. Lett.*, vol. 13, no. 8, pp. 869–871, Aug. 2001.

[9] R. Hernandez, A. Loayssa, and D. Benito, "Optical vector network analysis based on single-sideband modulation," *Opt. Eng.*, vol. 43, no. 10, pp. 2418–2421, Oct. 2004.

[10] Z. Tang, S. Pan, and J. Yao, "A high resolution optical vector network analyzer based on a wideband and wavelength-tunable optical single-sideband modulator," *Opt. Express*, vol. 20, no. 6, pp. 6555–6560, Mar. 2012.

[11] J. D. Bull, N. A. F. Jaeger, H. Kato, M. Fairburn, A. Reid, and P. Ghanipour, "40-GHz electro-optic polarization modulator for fiber optic communications systems," *Proc. SPIE*, vol. 5577, pp. 133–143, Sep. 2004.

[12] R. G. De Voe, C. Fabre, K. Jungmann, J. Hoffnagle, and R. G. Brewer, "Precision optical-frequency-difference measurements," *Phys. Rev. A*, vol. 37, no. 5, pp. 1802–1805, Mar. 1988.